Mixing Time Analysis of the Bottom Blown Steelmaking Ladle

A Thesis submitted
in Partial Fulfilment of the Requirements
for the Degree of

Master of Engineering
in
Mechanical Engineering

Submitted By

DEBASIS DE

Examination Roll No.:
M4MEC22031B

Under the Guidance of

Prof. Dipankar Syanyal
And
Prof. Sandip Sarkar

DEPARTMENT OF MECHANICAL ENGINEERING
FACULTY OF ENGINEERING & TECHNOLOGY
JADAVPUR UNIVERSITY
188, RAJA S.C. MULLICK ROAD, KOLKATA-700032, INDIA

November, 2022

DECLARATION OF ORIGINALITY AND COMPLIANCE OF ACADEMIC ETHICS

I hereby declare that the thesis entitled "**Mixing Time Analysis of the Bottom Blown Steelmaking Ladle"** contains literature survey and original research work by the undersigned candidate, as a part of his MASTER OF ENGINEERING IN MECHANICAL ENGINEERING studies during academic session 2020-2021. All information in this document have been obtained and presented in accordance with the academic rules and ethical conduct. I also declare that, as required by these rules of conduct, I have fully cited and referenced all the material and results that are not original to this work.

Name: **DEBASIS DE**

Examination Roll Number: **M4MEC22031B**

University Registration Number: **154330 of 2020-21**

Thesis Title: **Mixing Time Analysis of the Bottom Blown Steelmaking Ladle**

Signature: _____

FACULTY OF ENGINEERING & TECHNOLOGY
DEPARTMENT OF MECHANICAL ENGINEERING
JADAVPUR UNIVERSITY
KOLKATA

CERTIFICATE OF RECOMMENDATION

This is to certify that the thesis entitled "**Mixing Time Analysis of the Bottom Blown Steelmaking Ladle"** is a bona fide work carried out by Debasis De under our supervision and guidance in partial fulfilment of the requirements for awarding the degree of Master of Engineering in Fluid Mechanics & Hydraulic Engineering under Department of Mechanical Engineering, Jadavpur University during the academic session 2021-2022.

_____

Thesis Supervisor

Prof. Dipankar Syanyal

Professor

Department of Mechanical Engineering

Jadavpur University, Kolkata

_____

Thesis Co-Supervisor

Prof. Sandip Sarkar

Professor

Department of Mechanical Engineering

Jadavpur University, Kolkata

_____

Prof. Amit Karmakar

Head of the Department

Department of Mechanical Engineering

Jadavpur University, Kolkata

_____

Prof. Bhaskar Gupta

Dean

Faculty of Engineering and Technology

Jadavpur University, Kolkata

FACULTY OF ENGINEERING & TECHNOLOGY
DEPARTMENT OF MECHANICAL ENGINEERING
JADAVPUR UNIVERSITY
KOLKATA

Certificate of Approval

The foregoing thesis, entitled "**Mixing Time Analysis of the Bottom Blown Steelmaking Ladle**" is hereby approved as a creditable study in the area of computational fluid dynamics carried out and presented by Mr. Debasis De (Registration No. 154330 of 2020-21) in a satisfactory manner to warrant its acceptance as a prerequisite to the degree for which it has been submitted. It is noticed to be understood that by this approval, the under-signed do not necessarily endorse or approve any statement made, opinion expressed and conclusion drawn therein but approve the thesis only for the purpose for which it has been submitted.

Final Examination for Evaluation of the Thesis

Board of Members

_____ _____

_____

_____ _____

_____ _____

ACKNOWLEDGEMENTS

I would like to express my gratitude to my supervisor Prof. Dipankar Sanyal & co-supervisor Prof. Sandip Sarkar who guide me to finalize my thesis work and extraordinary support me throughout to complete the thesis work. My special and heartily thank to my co-supervisor Prof. Sandip Sarkar who encouraged and directed me the right path to carry out this thesis work. I am also deeply I would also like to thank my friends and family who support me and offered deep insight into the study.

Debasis De

Jadavpur University

Date:04/11/2022

Abstract

For worldwide production of quality steel, ladle refining is extensively adopted in the secondary steel making process. The processing enhances the productivity of primary steel making and the overall economics. When liquid steel is poured in the ladle, alloy elements are added and an inert gas is injected from the bottom of the ladle to ensure the required quality and cleanliness. The gas is introduced through plugs or nozzles of different diameters arranged in different configurations invoked at the different stages of the process. In the present two-dimensional axisymmetric, transient, turbulent-flow simulation study, three arrangements of argon gas injection have been considered injected at the different rates of 2, 4 and 6 l/s and the time necessary for producing a homogenous mixture side has been assessed. For a cell-centre based finite-volume study with hexahedral mesh and realizable k-ε turbulence model, a grid independence study has been carried for the selection of the mesh. A successful validation study with an existing numerical result for 20 l/s argon gas injected through a central plug has been performed. Two more configurations, one with an eccentric plug and another with symmetric arrangement of two central plugs, have been compared in a detailed numerical analysis. For the highest rate, the mixing time has been extracted to be the least for all the arrangements. The longest and the least mixing times have been predicted respectively with the central plug and the twin-plug configurations. It would be interesting to study the effect of invoking eccentric and twin-injections in sequential phases over the processing time.

Contents

Chapter 6

Chapter 7

Chapter 8

Chapter 9

Nomenclature

English symbol

α_q- Volume fraction of q phase

ρ_q-Density of q phase

$\vec{u}_q$- Velocity of q phase

∇p-Gradient of pressure

$\vec{F}_{lift,q}$- Lift force

$\vec{F}_{td,q}$- Turbulent dissipation force

$\bar{\bar{\tau}}_q$- Stress tensor

$\boldsymbol{\lambda}_q$- Bulk viscosity of q phase

μ_q - Effective viscosity of q phase

G_k- Turbulence kinetics energy due fluid mean velocity

G_b- Turbulent kinetic energy due to bouncy

Pr_t- Turbulent Prandtl number

β- Coefficient of thermal expansion

μ_t- Turbulent viscosity

h_q- Specific enthalpy of q phase

q_q - Heat flux of q phase

Q_{pq}Heat exchange between the phases

Chapter 1

1.1 Introduction

Steel is called most useful and inexpensive metal in the world and as per Steel association statistical data of 2018 total steel produce with the help of EAF is more than 445 million ton which is 12.3% more than previous year. Steel is extracted from iron ore, a compound of iron, oxygen and other minerals that occur in nature. The raw materials for steelmaking are mined and then transformed into Steel are primarily produced using one of two methods: Blast Furnace or Electric Arc Furnace (EAF). The blast furnace is the first step in steel production from iron oxides. At first blast furnaces appeared in the 14th century and produced rate was one ton per day. Even though equipment is improved and higher production rates can be achieved, the processes inside the blast furnace remain the same. The blast furnace uses coke, iron ore and limestone to produce pig iron or crude iron which has a very high carbon content, typically 3.8–4.7%[1]. First electric arc furnaces (EAFs) is used to produced steel which was first in the late 19th Century. The use of EAFs has been expanded day by day and now in present over 70 percent of steel production in the United States with the help of first electric arc furnaces (EAFs). The main different of EAF with the blast furnace is quality of steel as describe above the blast furnace produced pig iron but electric arc furnaces (EAFs) is used to produced molten steel with the help of electrical current to melt scrap steel or pig iron, to produce molten steel which has carbon content, typically 3.8–4.7%[1]. In the above discussed part are all related with steel making process but now a day due to high demands on steel quality and consistency in its properties various kinds of liquid steel treatment developed in which case ladle play a important role to produce such kind of quality steel and above mentioned are collectively known as secondary steelmaking. Now a day the secondary steelmaking is the heart of the production steps of modern steel making shops.

1.2 Literature Review

Ladle is play a important role to produce high quality steel so day after day increased application of ladle to produce quality steel in this regards number of investigate carried out numerical simulation and model experiment on EAF with different configuration. Q. Cao[2] mathematically invested of fluid flow and slag-steel interface behaviour of multi-phase flow domain with the help of Euler-Euler and Euler-Lagrange modelling approaches and compares numerical result with water model experiment result to perform comparisons which approach is more accurate Euler-Euler or Euler-Lagrange for multi-phase flow domain. Liu F[3] was carried out numerical simulated and water model experiment investigation of flow field and stirring effect of different kind of bottom blowing of arrangement on 75 t and it was shown bottom blowing could stir molten steel better compare with no bottom blowing arrangement . Haiyan[4] was carried out numerical simulation with different plug position and different gas flow rate to observed effect of plug position and gas flow rate on mixing time of the furnace. Finally an optimum bottom blowing arrangement was determined Electric Arc Furnace. Dia[5] was carried out numerical simulated of multi-phase model in an industrial Single Snorkel Refining Furnace (SSRF) and analysis density, bubble size & velocity also analysis effect of snorkel immersion depth (SID) on mixing time, circulation rate and flow parameters analysis. Urióstegui-Hernández[6] have been carried out numerical simulation on 50-t steel making ladle and Euler-Euler model used to analysis in the three phase fluid flow characteristic and thermal behaviour of liquid steel and model is validated by particle image velocimetry (PIV). Haiyan[7] have been carried out numerical simulation to find out the effect of plug position angle on mixing time and it was observed that for dual plug when plug angle

increasing from 45^0 to 90^0 mixing time increasing but which it position angle change from 90^0 to 180^0 it decrease due the stirring energy consumed decreased by the collision and interaction from two plumes. M. Che[8] have been carried out numerical simulation on ladle and analysis effect plug position and position angle on mixing time in the ladle and conclude that when plug position half of ladle bottom radius and plug position angle 45^0 then optimum mixing time observed. Wei[9] analysis the effect of bottom gas pulsing on ladle mixing and velocity distribution and it has been observed that due to bottom pulsing gas injection dead zone and mixing time signification decreased and improved flow velocity

1.3 Present Work

In the present study, analysis the effect of gas flow rate on fluid flow properties such as mixing time, velocity distribution, turbulent kinetics energy, turbulent dissipation rate distribution when argon gas injected from the bottom of the ladle with gas flow rates are 2 L/Sec, 4 L/Sec & 6 L/Sec. In the present work analysis effect of plug position of the above properties when argon gas flow rate kept 6 L/Sec and finally analyse the thermal behaviour of liquid steel in the ladle with same gas flow rate.

Chapter 2

2.1 Physical Model

Table 2.1. The dimensions of the ladle and other parameters used in the numerical simulation

Physical Properties	Value
Diameter of ladle (up)	3100 mm
Diameter of ladle (down)	2660 mm
Height of ladle	3350 mm
Diameter of the plug	92 mm
Gas flow rate for each plug	2 L/, 4 L/s, 6L/s
Density of liquid steel	7020 kg/m^3
Density of argon gas	0.568 kg/m^3
Viscosity of steel	0.006 $kg/(m^2\text{-}s)$
Viscosity of argon gas	$2.13x10^{-5} kg/(m^2\text{-}s)$
Interfacial Tension Between Steel and Gas	1.4 N/m

The above table 2.1 showed ladle dimension where in the present study used 2-D model for numerical simulation. In the ladle bottom diameter, outlet and height are 2660mm, 3100mm and 3350mm. In the present study gas is injected from bottom plug where plug diameter is 92mm and simulation work analysis with different plug configuration as per below figure 2.1.

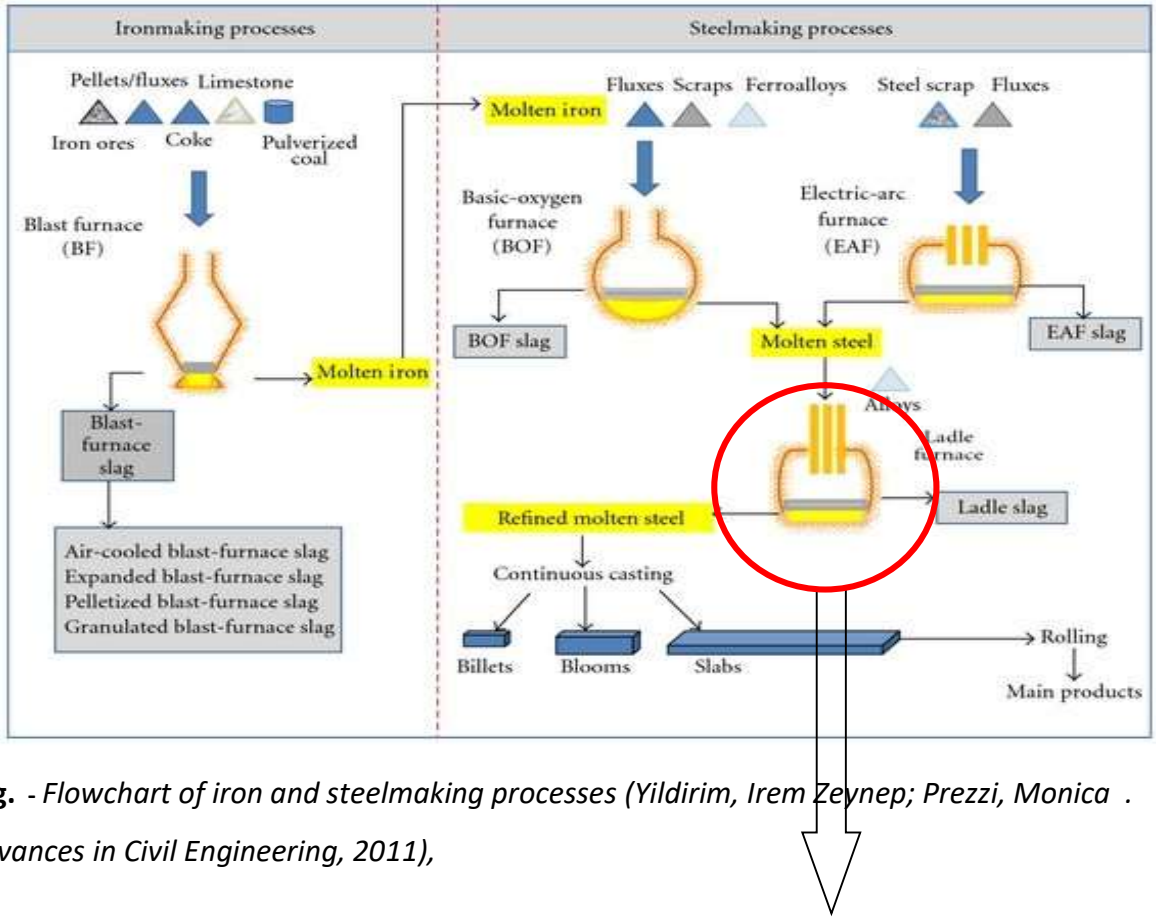

Fig. *- Flowchart of iron and steelmaking processes (Yildirim, Irem Zeynep; Prezzi, Monica . Advances in Civil Engineering, 2011),*

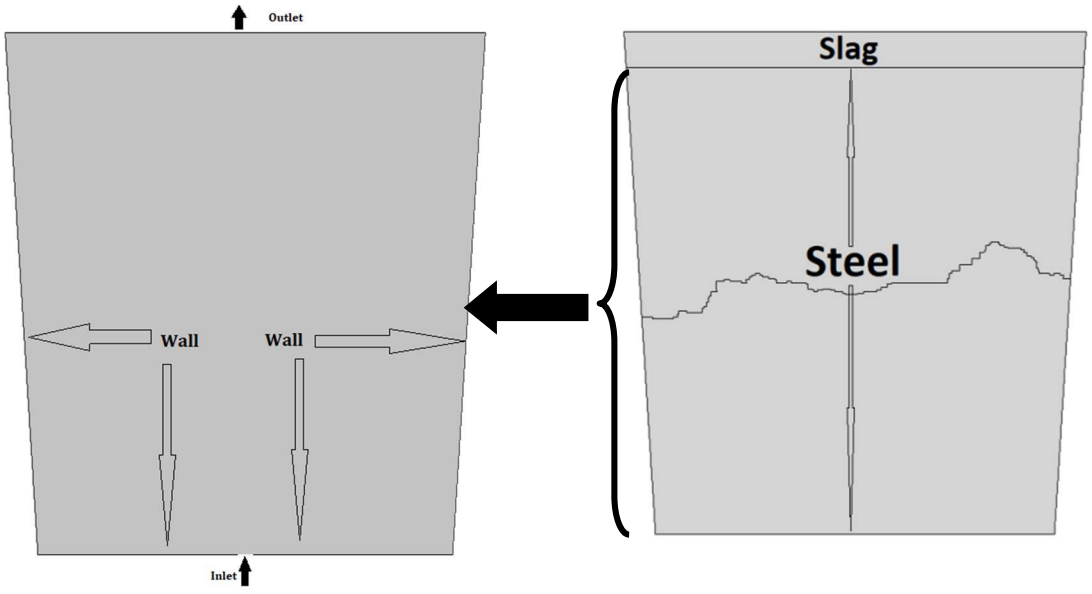

Fig. 2.1 Geometric representation the ladle and bottom –blowing nozzle arrangement

2.2 Grid Generation

The numerical domain and mesh configuration of the present study in shown in below figure 2.2. In the present study a complete hexahedral mesh has been generate of mesh size is set 10 mm and total number of elements and nodes are 96432 and 97056. Ansys fluent 2020 R1 software is used to perform the numerical simulation. Average orthogonal quality and skewness of the generated mesh are 0.99934(bad value =0; ideal quality value = 1) and 0.90000 in the present model.

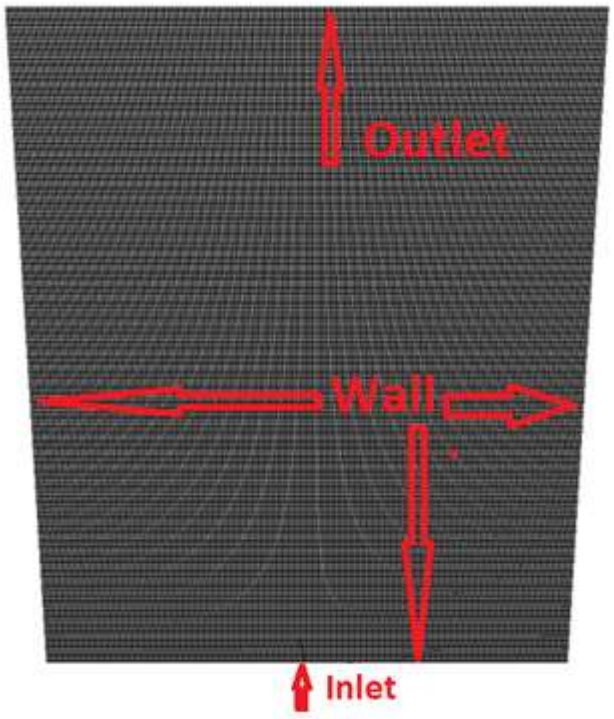

Fig. 2.2: Details grid schemes of numerical simulation mode

2.3 Assumptions

(1) Electromagnetic forces or chemical reactions have not been considered in the present study.

(2) The gas phase was consider as compressible and Newtonian fluid, and liquid molten steel was consider as incompressible and Newtonian fluid.

(3) Liquid and gases flow were considered two-dimensional, transient and turbulent-flow model.

(4) During simulation viscosity and surface tension all the phases were assumed constant.

(5) A no-slip wall boundary condition was applied to all of model walls.

Chapter 3

3.1 Initial and Boundary Condition

Initially liquid steel rest on the ladle and no gas flow take place from bottom plug. No-slip and standard wall function used at the bottom and side wall. Outflow boundary condition applied at the outlet of the ladle. Velocity inlet boundary condition applied at the inlet of the nozzle. Inlet velocity u_q have been calculated with the help of inlet gas flow rate [2].

3.2 CFD model & Governing Equations

In the present study Euler model approach have been applied. In this approach, VOF method is applied to performed simulation work of transient two-dimensional argon gas, steel two phase fluid flow in EAF. VOF model is useful for the study to focus on interface tracking for two or more phase simulation. Each phase which has to be added in the model is represent the volume of fraction of the added phase variable is introduced, which represent the volume fraction of the phase in the computational cell. In each simulated domain sum of the all-phase volume of fraction is unit [12] . The tracking of the interfaces among all the phases is accomplished by solving the continuity equation for the volume fraction of phases. The continuity equation for the q^{th} phase is mentioned below [12].

$$\frac{1}{\rho}\left[\frac{\partial(\alpha_q \rho_q)}{\partial t} + \nabla \cdot (\alpha_q \rho_q \vec{u}_q)\right] = 0$$

In the above α_q volume fraction of q^{th} phase and as per mentioned above $\sum_{q=1}^{n} \alpha_q = 1$

The momentum Equation

The momentum equation is solved through the domain and resulting velocity shear among the phases. The momentum equation given below [6]–

$$\frac{\partial}{\partial t}\left(\alpha_q \rho_q \vec{u}_q\right) + \nabla.\left(\propto_q \rho_q \vec{u}_q \vec{u}_q\right) = -\alpha_q \nabla p + \nabla.\bar{\bar{\tau}}_q + \alpha_q \rho_q \vec{g} + \sum_{p=1}^{n} \vec{R}_{pq} + \left(\vec{F}_{lift,q} + \vec{F}_{td,q}\right)$$

Where p is static pressure g is gravitational acceleration, $\vec{F}_{lift,q}$ & $\vec{F}_{td,q}$ are lift force and turbulent dispersion force, $\vec{R}_{pq}$ is the force interaction between the phases, $\bar{\bar{\tau}}_q$ is known as stress sensor which is defined as-

$$\bar{\bar{\tau}}_q = \alpha_q \mu_q \left(\vec{v}_q + \nabla \vec{u}_q^T\right) + \alpha_q \left(\lambda_q - \frac{2}{3}\mu_q\right) \nabla.\vec{u}_q \bar{I}$$

Where λ_q is bulk viscosity and μ_q is effective viscosity of the q phase.

k-ε Realizable Turbulence Model

The realizable k-ϵ turbulent model chosen to solve turbulent multi-phase problem. For wall function we have used standard wall function to solve near wall turbulent flow. Equations (6) and (7) are used to k & ϵ [12].

$$\frac{\partial(\rho k)}{\partial t} + \frac{\partial(\rho k u_j)}{\partial x_j} = \frac{\partial}{\partial x_j}\left[\left(\mu + \frac{\mu_t}{\sigma_k}\right)\frac{\partial k}{\partial x_j}\right] + G_k + G_b - \rho\varepsilon \quad \text{..... (6)}$$

$$\frac{\partial}{\partial t}(\rho\epsilon) + \frac{\partial(\rho\epsilon u_j)}{\partial x_j} = \frac{\partial}{\partial x_j}\left[\left(\mu + \frac{\mu_t}{\sigma_\epsilon}\right)\frac{\partial \epsilon}{\partial x_j}\right] + \rho C_1 S_\epsilon - \rho C_2 \frac{\epsilon^2}{k+\sqrt{\gamma\epsilon}} +$$

$$C_{1\epsilon}\frac{\epsilon}{K}C_{3\epsilon}G_b \text{..... (7)}$$

Where,

$$C = max\left[0.43, \frac{n}{n+5}\right],\ n = S\frac{K}{\epsilon},\ s = \sqrt{2S_{ij}S_{ij}},\ \text{and}\ S_{ij} = \frac{1}{2}\left(\frac{\partial u_j}{\partial x_i} + \frac{\partial u_i}{\partial x_i}\right)$$

In the above equation G_k represents the generation of turbulence kinetics energy due to fluid mean velocity gradient and it's calculate as below-

$$G_k = \rho u_i' u_j' \frac{\partial u_j}{\partial x_i}$$

G_b is represent the turbulent kinetic energy due to buoyancy, which is define as below-

$$G_b = \beta g_i \frac{\mu_t}{Pr_t}\frac{\partial T}{\partial x_i}$$

Where Pr_t represent turbulent Prandtl number which is 0.85 for k- ϵ [12] model .g_i is gravitational acceleration in the direction. β is coefficient of thermal expansion, which is defined as-

$$\beta = -\frac{1}{\rho}\left(\frac{\partial \rho}{\partial T}\right)P$$

μ_t is define as eddy viscosity which is define as-

$$\mu_t = \rho C_\mu \frac{k^2}{\epsilon}$$

The degree of which ϵ is affected by the buoyancy is determined by the constant$C_{3\epsilon}$, which is determine by given below –

$$C_{3\epsilon} = \tanh\frac{v}{u}$$

Where v and u velocity of components parallel and perpendicular to the gravitational acceleration direction.

The model constants are given by $C_{1\epsilon} = 1.44, C_2 = 1.9, \sigma_k = 1.0, \& \sigma_\epsilon = 1.2$[12]

Energy Equation

Energy equation [6] of Euler multi-phase model is given as per below-

$$\frac{\partial}{\partial t}(\alpha_q \rho_q h_q) + \Delta \cdot (\alpha_q \rho_q h_q \vec{u}_q) = \alpha_q \frac{\partial p_q}{\partial t} + \bar{\bar{\tau}} : \nabla \vec{u}_q - \nabla \cdot \vec{q}_q + \sum_{p=1}^{n} (Q_{pq})$$

Where hq is specific enthalpy J/Kg of q phase q_q is heat flux w.m^{-2} of q phase and Q_{pq} is heat exchange in joules between the phase.

Mixing Time Equation

The mixing process is simulated by introducing a tracer into the ladle when a steady-state flow regime is reached, and then monitoring the species concentration with respected to the time. A species transport model is used to analysis the mixing beaver of the domain

$$\frac{\partial}{\partial t}(\rho C) + \nabla.(\rho \vec{u} C) = \nabla.\left(\frac{\mu_t}{Sc_t}(\nabla C)\right)$$

where μ_t is the turbulent viscosity. Sc_t is the turbulent Schmidt number, the default Sc_t is 0.7, and C is the local mass fraction of tracer in liquid steel. The mixing time is defined the time required to get 95% level of concentration, which id define that the concentrations C(t) at all monitoring points in the bath are within ±5% deviation of the homogeneous

Concentration value, C(∞).

3.3 Grid Independence Test

Grit independence test carried out to check the accuracy of the model and optimum point of grid size identify. In the present study we have been carried out grid independence test with seven different mesh size and its observed that for 10mm grid size is optimum grid size as different of surface velocity magnitude less than 1% as shown in the below table 3.3.

Table 3.3: Mesh statistics for grid independence test

Sl No.	Mesh Elements Size(mm)	Cell count	Surface Velocity magnitude(m/s)	% Different
1	9.5	106600	0.45061	--
2	10	96432	0.45058	0.007
3	10.5	87954	0.44548	1.132
4	11	79605	0.44018	1.19
5	11.5	73000	0.43509	1.156
6	12	67200	0.42875	1.457
7	12.5	61870	0.42202	1.57

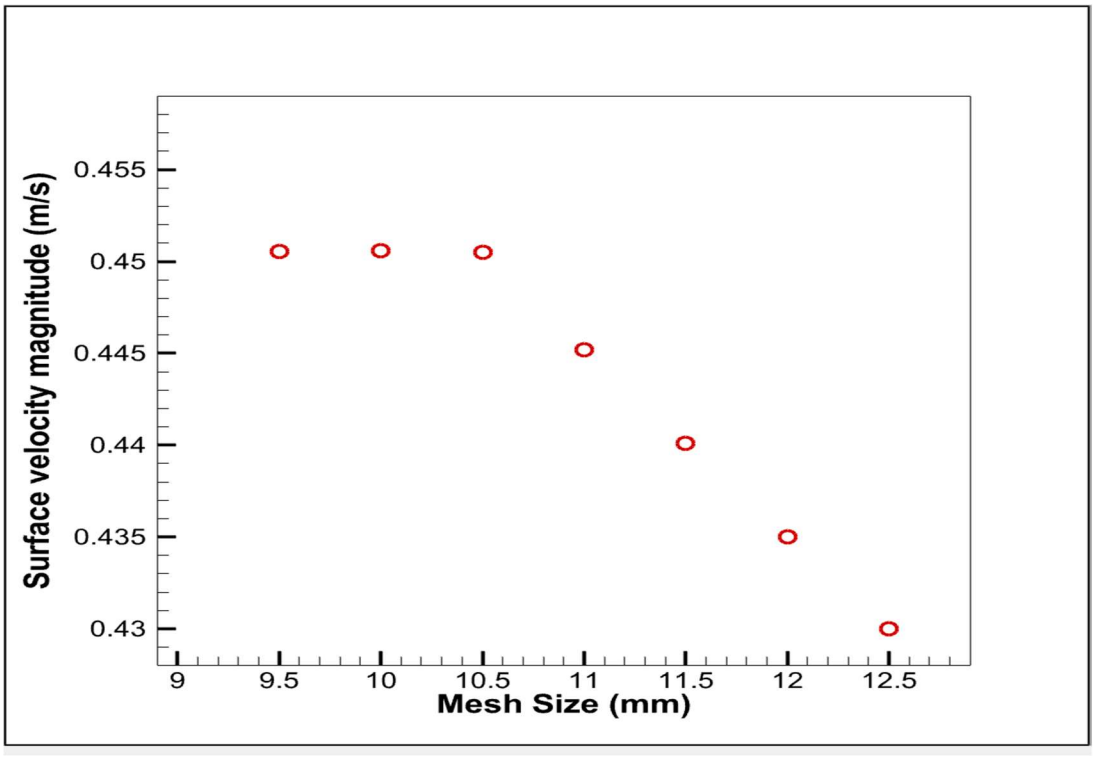

Fig. 3.3: Results from grid convergence study showing the dependence of surface velocity on the number of mesh elements.

Chapter 4

4.1 Solution Methodology

Pressure-base solver used to solve the governing equation using CFD package FLUENT 2020 R1[10] software. This package runs on a cell-cantered based finite volume method to discredit the governing equation and SIMPLE scheme used for pressure velocity coupling and the volume fraction equation is solved using first order upwind.

4.2 Pressure Base Solver

In the pressure-based solver, the governing equations are solved sequentially i.e. Governing equation for the variables such as u, v, w, p, T, k etc. are solved one after another and the solution algorithm for sequential pressure-based solver is represented below.

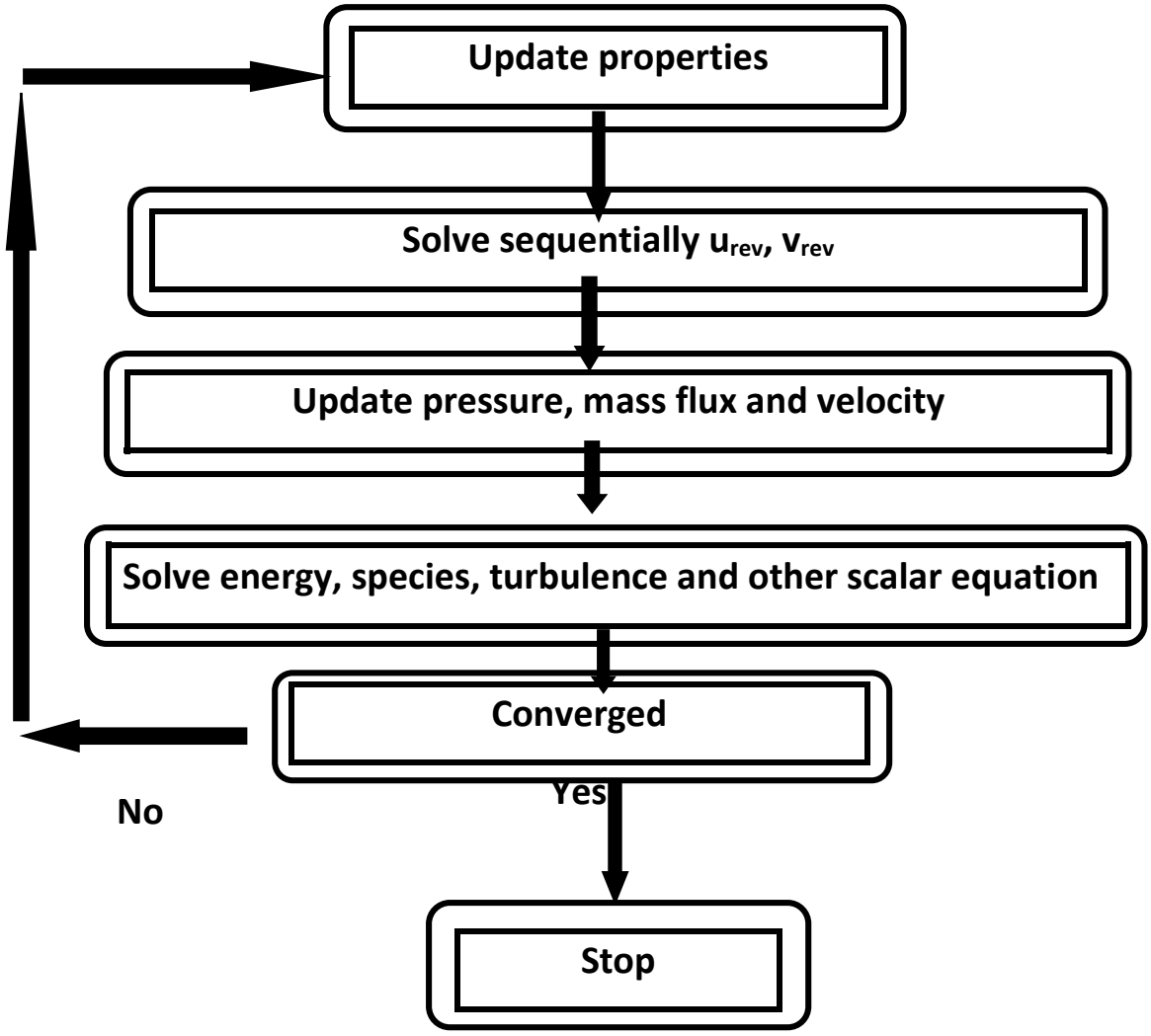

Fig.-4.2: Overview of the Pressure-Based Segregated Algorithm.

Chapter 5

5.1 Model Validation

Model validation is an important assignment to validate current numerical simulation with reference study. In the present study numerical simulation is validated with the numerical result of literature [13]. To validate the present model 20 L/Sec gas flow rate used to compare the result with reference data and compare ladle centre line velocity variation and mixing time behaviour with the reference data. It is seen from below fig.5.1a & b that the simulation result agrees well with the literature [13] within a maximum deviation of 3%.

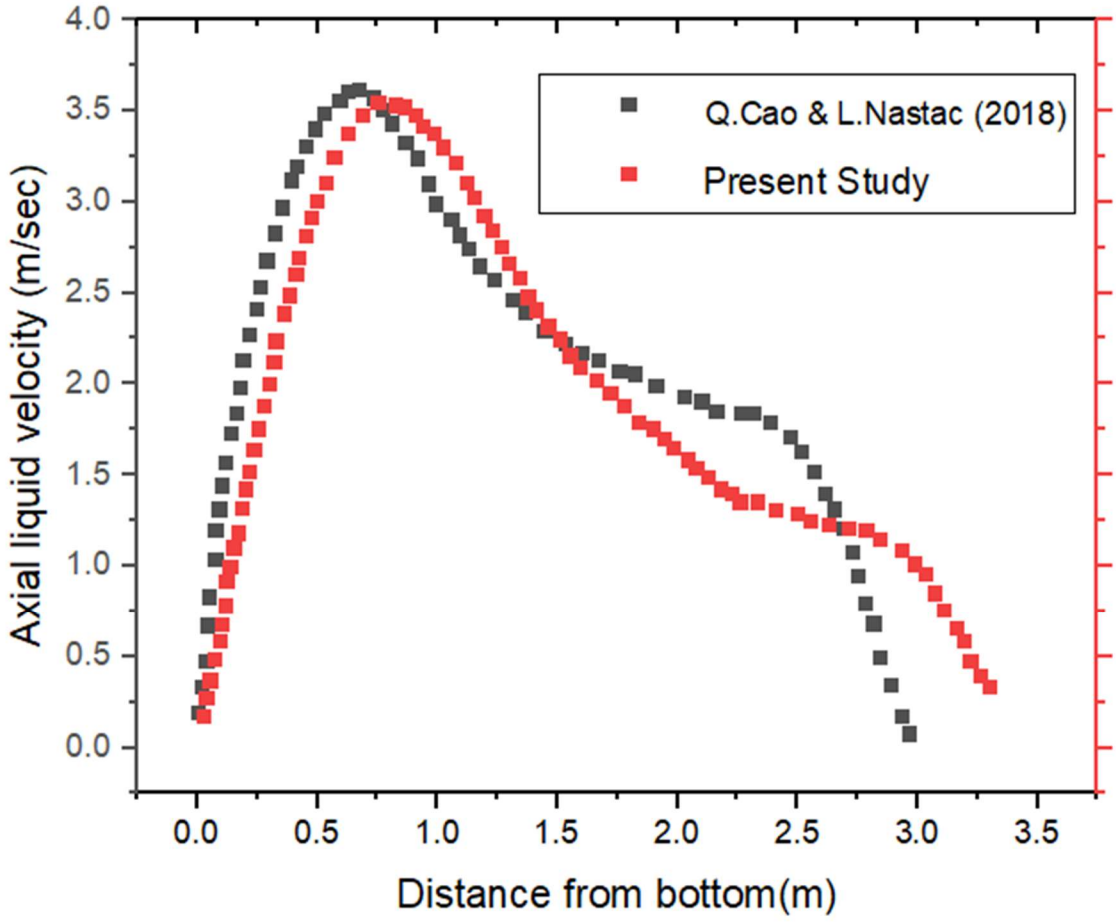

Fig. 5.1a : Comparison of the axial liquid velocity with the numerical results of Q.Cao & L.Nastac[13].

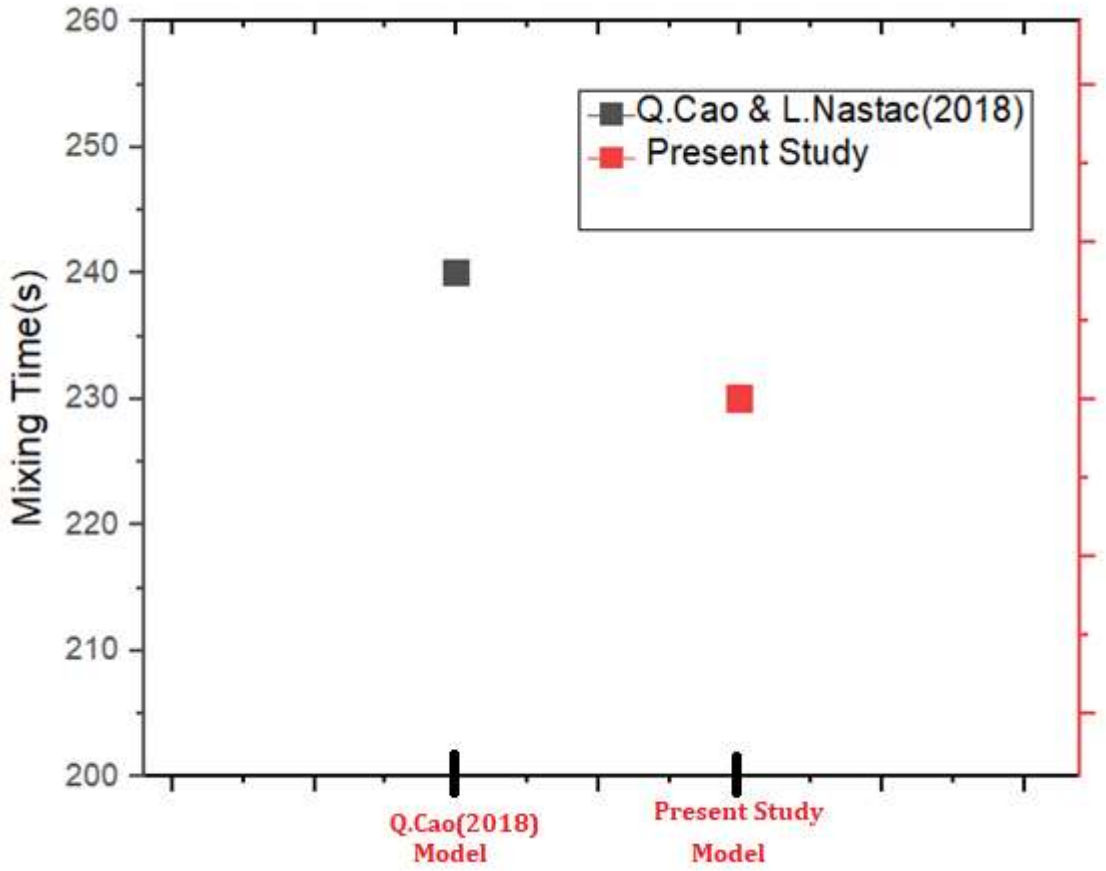

Fig. 5.1b : Comparison mixing time with the numerical results of Q.Cao & L.Nastac[13].

Chapter 6

6.1 Effect of Bubble Size on Gas Volume Fraction Distribution

In the present study observed effect of the bubble diameter in gas volume distribution and in the study set 1mm and 10mm bubble size in the Euler – Euler model and 20 L/Sec gas flow rate apply without change the other parameters setting in the simulation it has been observed that with decrease the bubble size gas volume fraction increasing which have been displayed in figure 6.1. In the below figure it's observed that with decreased bubble dia. more dispersed pattern and easy to penetrated through the mould and tendency of less bouncy and present work is good agree with the simulation work [11] and subsequent study apply bubble size in the Euler model.

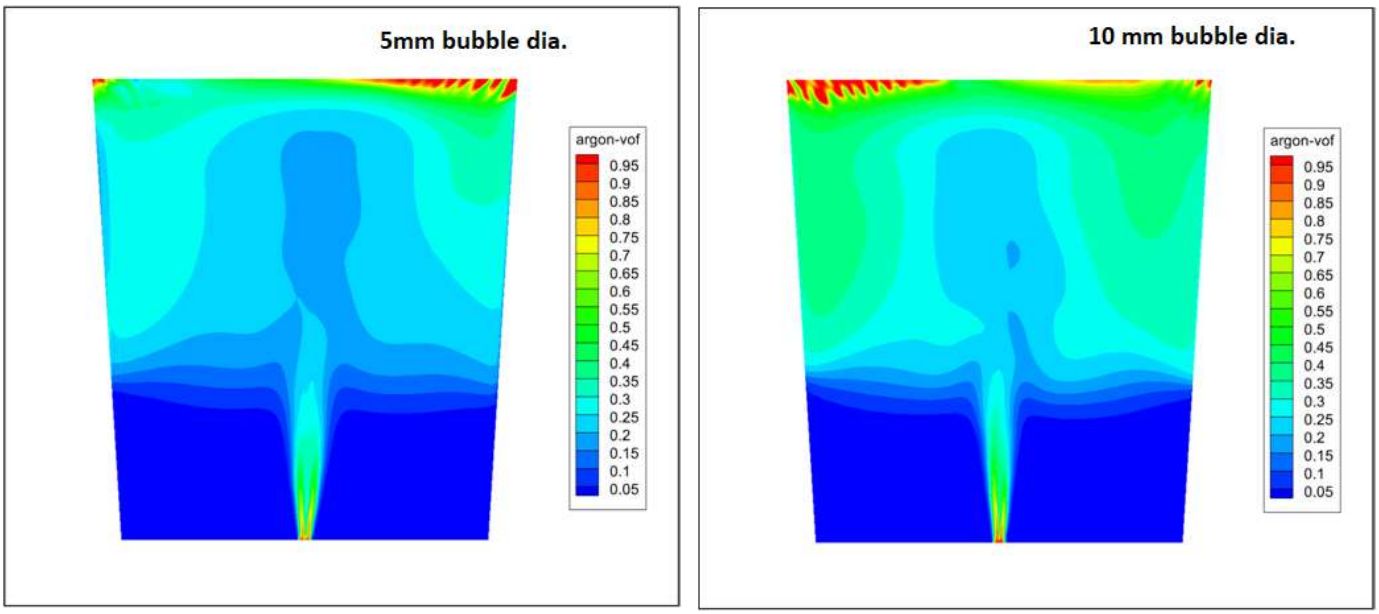

Fig. 6.1 : The effect of gas volume fraction distribution inside the Ladle for bubble diameters 5 mm & 10 mm

6.2 Axial Flow Velocity Distribution

In the figure 6.2 depicted the velocity distribution along the centre of plug /ladle. It is observed that with the increase gas flow rate velocity of centre line increase from 1m/sec to 2m/sec when gas flow rate increase 2L/Sec to 6 L/Sec. It also observed that velocity suddenly increased from bottom of the ladle and become maximum approximate 0.5 m from bottom of the ladle after that it is gradually decreased up to the ladle outlet.

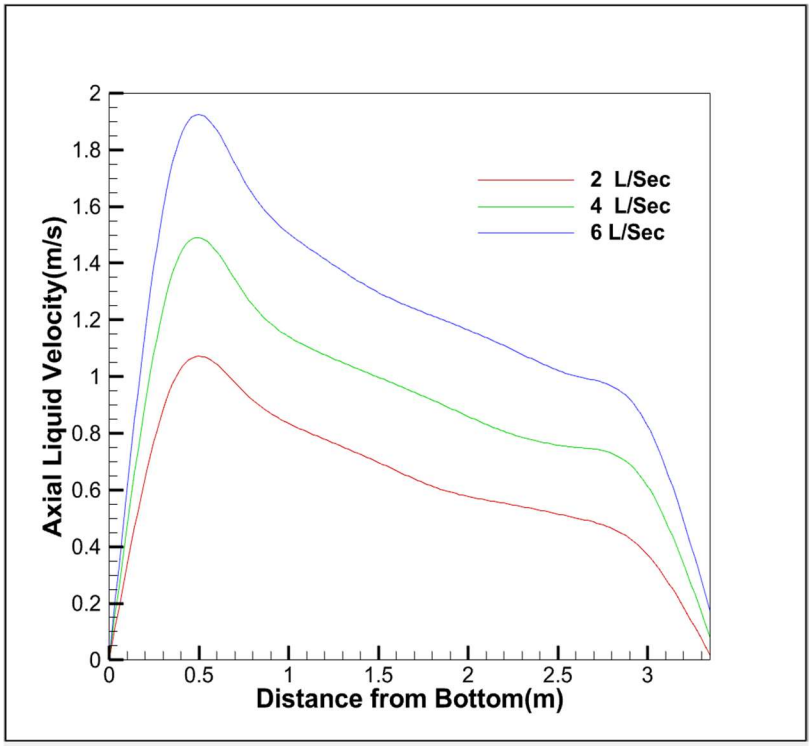

Fig. 6.2: Axial Flow Velocity Distribution for gas flow rate 6 L/Sec, 4 L/Sec & 2 L/Sec

6.3 Axial Turbulence Kinetic Energy Distribution

In the figure 6.3 depicted the turbulent kinetic energy distribution along the centre of plug /ladle. It is observed that with the increase gas flow rate turbulent kinetic energy of centre line increase from 0.12 m^2/sec^2 to 0.44 m^2/sec^2 when gas flow rate increase 2 L/Sec to 6 L/Sec. It also observed that turbulent kinetic energy suddenly increased from bottom of the ladle and become maximum approximate 0.5 m from bottom of the ladle after that it is gradually decreased up to the ladle outlet.

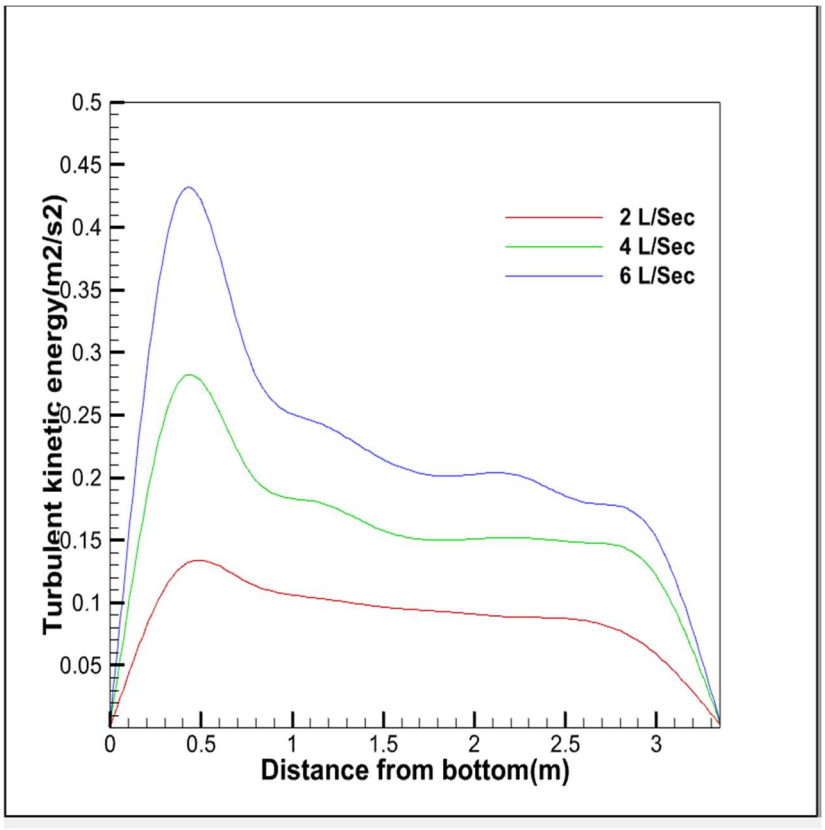

Fig. 6.3 : Axial Flow turbulent kinetic energy Distribution for gas flow rate 6 L/Sec, 4 L/Sec & 2 L/Sec

6.4 Axial Turbulence dissipation Rate Profile

In the figure 6.4 depicted the turbulence dissipation rate along the centre of plug /ladle. It is observed that with the increase gas flow rate turbulence dissipation rate of centre line increase from 0.5 m^2/sec^2 to 5.2 m^2/sec^2 when gas flow rate increase 2 L/Sec to 6 L/Sec. It also observed that turbulence dissipation rate suddenly increased from bottom of the ladle and become maximum approximate 0.5 m from bottom of the ladle after that it is gradually decreased up to the ladle outlet.

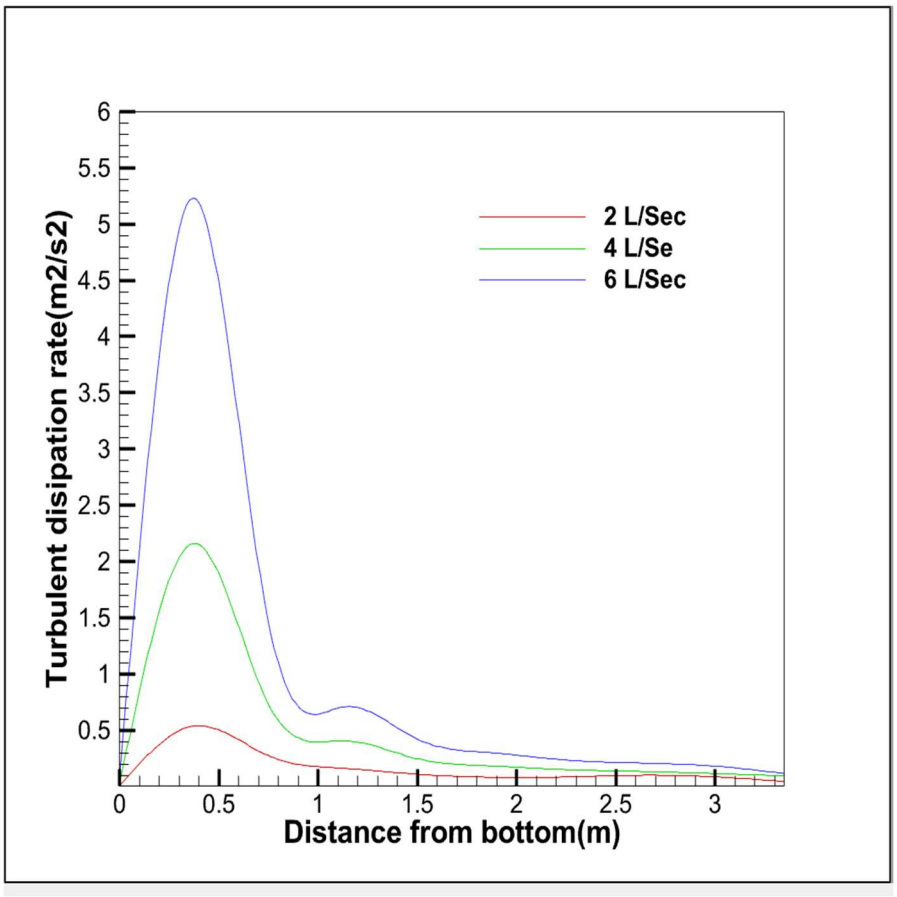

Fig. 6.4 : Axial Flow turbulence dissipation rate distribution for gas flow rate 6 L/Sec, 4 L/Sec & 2 L/Sec

6.5 Radial Flow Velocity Distribution

In figure 6.5 pictured radial velocity distribution of the fluid domain from 1.5m of furnace bottom of the given gas flow rate and it have been observed that velocity at nozzle position is very high and a small velocity observed near the nozzle position which is decreased left and right side accordingly. In the figure it also observed that peak velocity at nozzle position vary from 0.9 m/sec to 1.26 m/sec and left and right position of the nozzle it is become zero which is Validated the result with from literature[14].

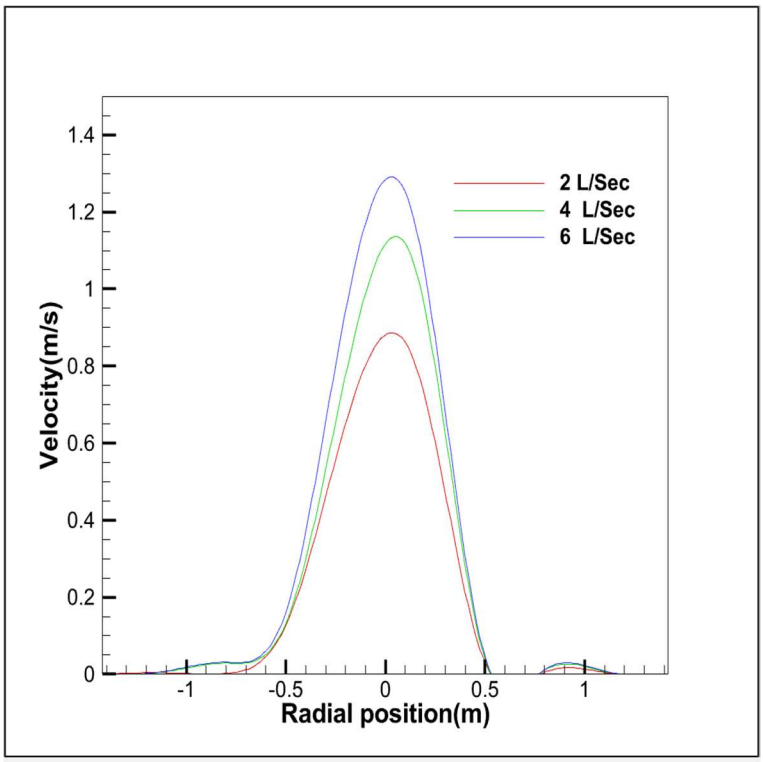

Fig. 6.5 : Radial velocity distribution from 1.5 m of ladle bottom for gas flow rate 6 L/Sec, 4 L/Sec & 2 L/Sec

6.6 Radial Turbulence Kinetic Energy Distribution

In figure 6.6 pictured radial turbulence kinetic energy distribution of the fluid domain from 1.5m of furnace bottom of the given gas flow rate and it have been observed that Turbulence Kinetic Energy plug position suddenly rise and a small turbulence kinetic energy distribution observed near the nozzle position which is decreased left and right side accordingly and become zero at boundary wall. In the figure it also observed that peak turbulence kinetic energy distribution at plug position of 1.5m position varies from 0.11 m^2/sec^2 – 0.24 m^2/sec^2 when gas flow rate vary 2L/Sec to 10 L/Sec.

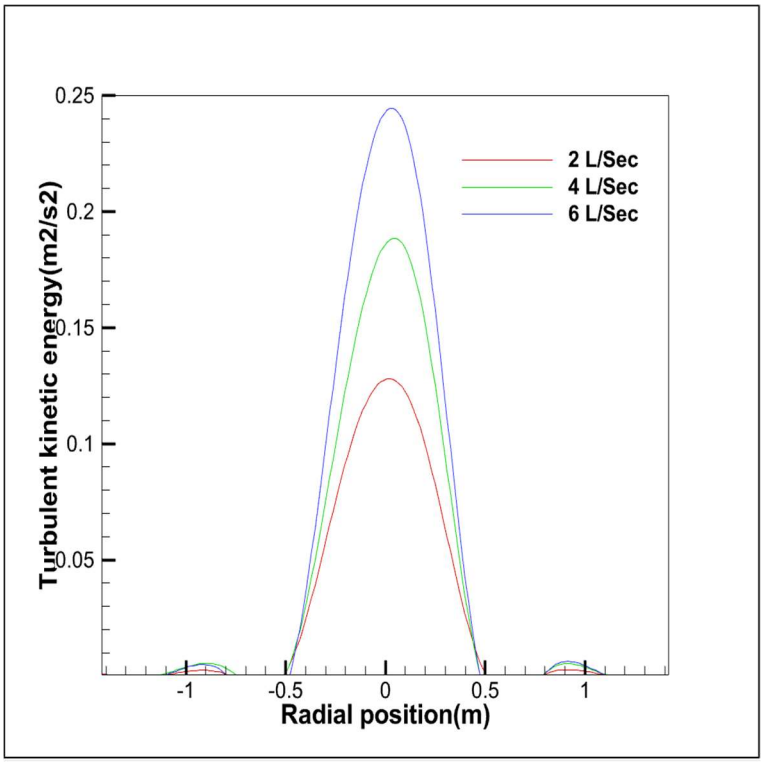

Fig. 6.6 : Radial turbulence kinetic energy distribution from 1.5 m of ladle bottom for gas flow rate 6 L/Sec, 4 L/Sec & 2 L/Sec

6.7 Radial Turbulence dissipation Rate Profile

In figure 6.7 pictured radial turbulence dissipation rate distribution of the fluid domain from 1.5m of furnace bottom of the given gas flow rate and it have been observed that turbulence dissipation rate plug position is suddenly increase and a small turbulence dissipation rate observed near the nozzle position which is decreased left and right side accordingly. In the figure it also observed that peak turbulence dissipation rate at nozzle position of 1.5m position vary from $0.1m^2/sec^2$-$0.28m^2/sec^2$ which become zero at boundary wall.

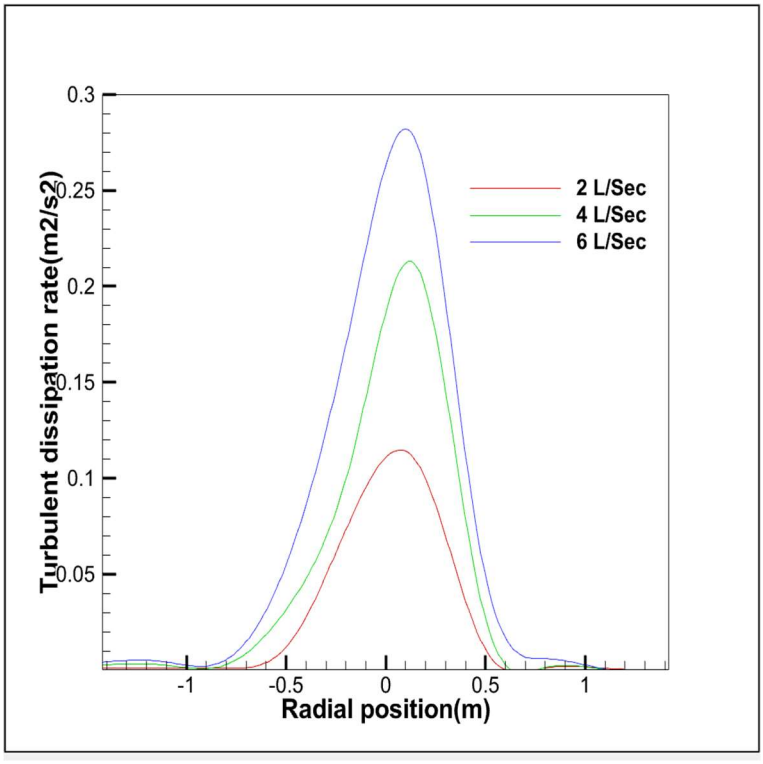

Fig. 6.7 : Radial turbulence dissipation rate distribution from 1.5 m of ladle bottom for gas flow rate 6 L/Sec, 4 L/Sec & 2 L/Sec

6.8 Contour Analysis for 6L/Sec Gas Flow Rate

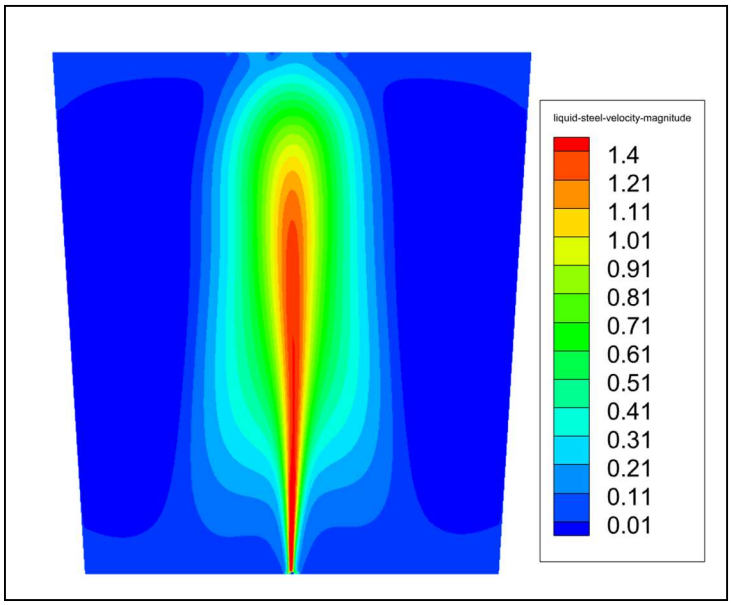

Fig. 6.8a: Velocity Contour

In the velocity contour it observed that at nozzle position stronger velocity distribution observed and it gradually decrease left and right side of the plug position which become zero at boundary wall.

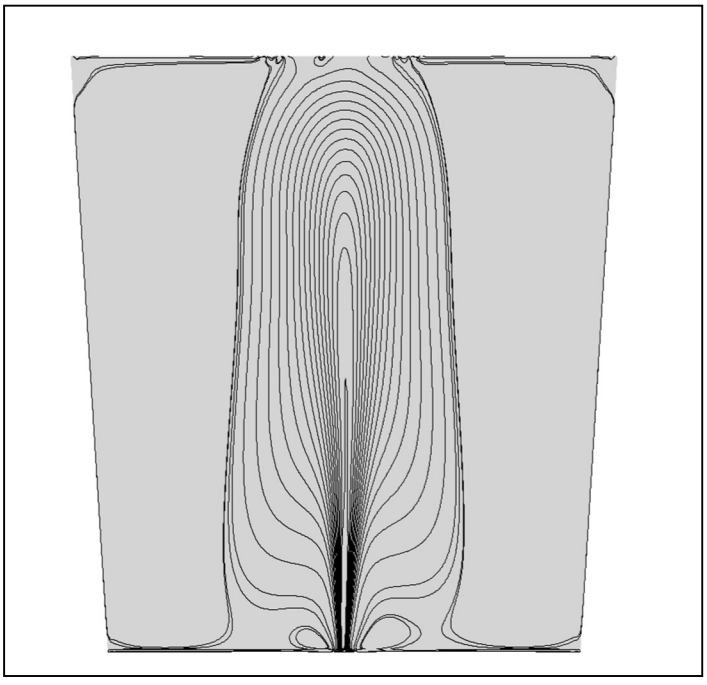

Fig. 6.8b: Stream Line Contour

In the stream line distribution it observed that at plug position stronger stream line pattern observed and it have been decreased left and right side of plug position

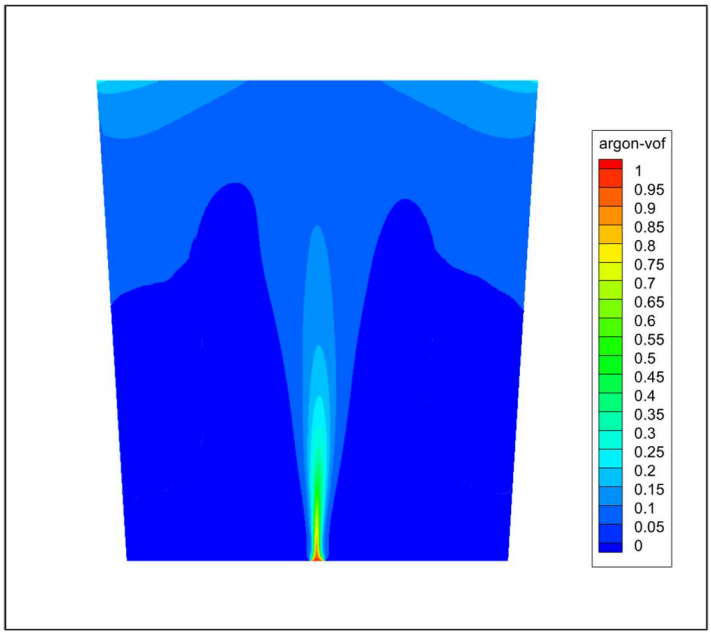

Fig. 6.8c: Gas Volume fraction Contour

In the gas volume contour of argon gas shown that argon gas volume distribution gradually increased from bottom nozzle position and is maximum value observed at outlet of the furnace.

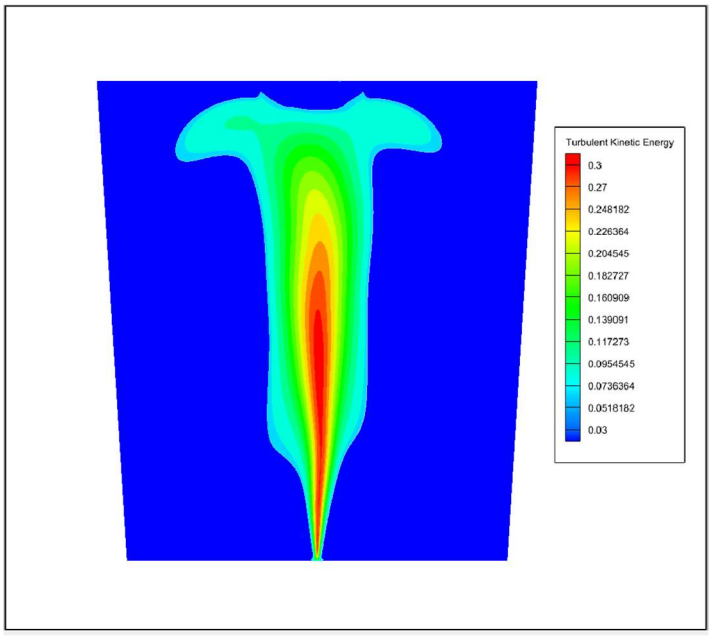

Fig. 6.8d: Turbulent Kinetics Energy Contour

In the Turbulent Kinetics Energy contour it observed that at nozzle position stronger Turbulent Kinetics Energy distribution observed and it gradually decrease left and right side of the plug position which become zero at boundary wall as well as the outlet of the ladle.

6.9 Mixing Behaviour for Different Gas Flow Rate

In the below figure 6.9b-6.9d displayed tracer response curve of six point (Fig.6.9a) and mixing time consider with 95% concentration evaluate all six points with different bottom argon gas flow rate. From below figure it is clear that with increased inject argon gas flow rate mixing time deceased so a reverse relationship build between gas flow rate and mixing time. In the present study it is observed that for 2L/Sec maximum mixing time observed and subsequently decreased for 6L/Sec. In the present study it is observed that mixing time for 2L/Sec, 4L/Sec & 6L/Sec are 1775 Sec ,1400 Sec & 1000 Sec .The numerical simulation value is good agree with the simulation work[13].

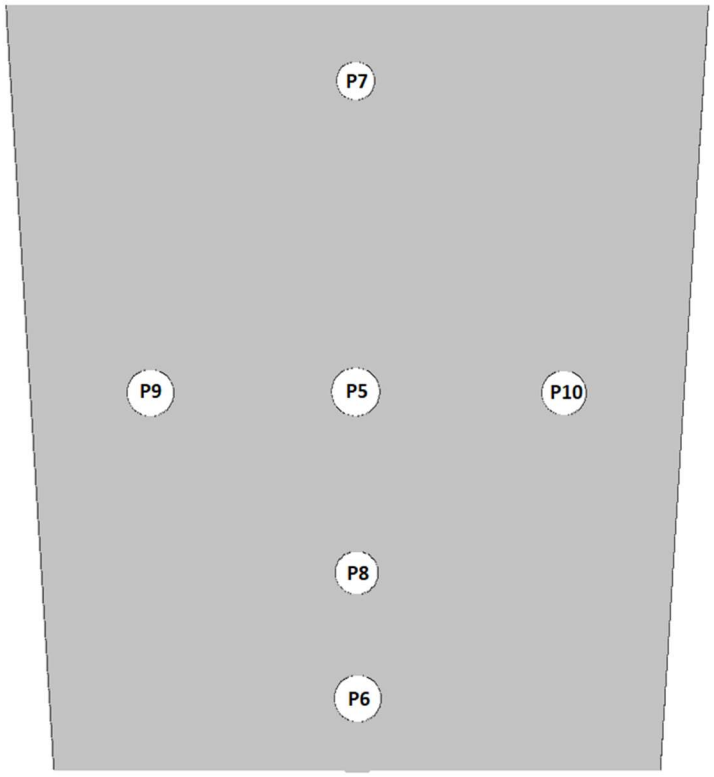

Fig. 6.9a : Mixing monitoring location inside the ladle

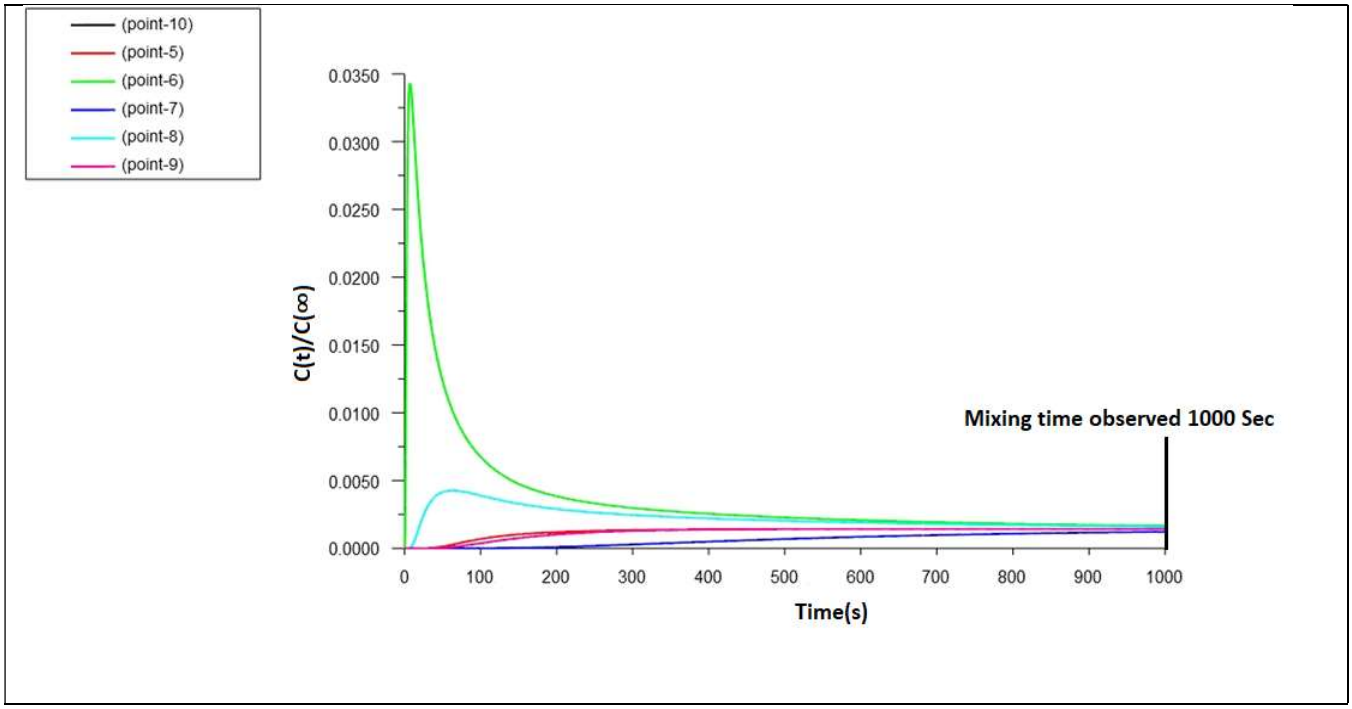

Fig. 6.9b: Mixing time for gas flow rate 6 L/Sec

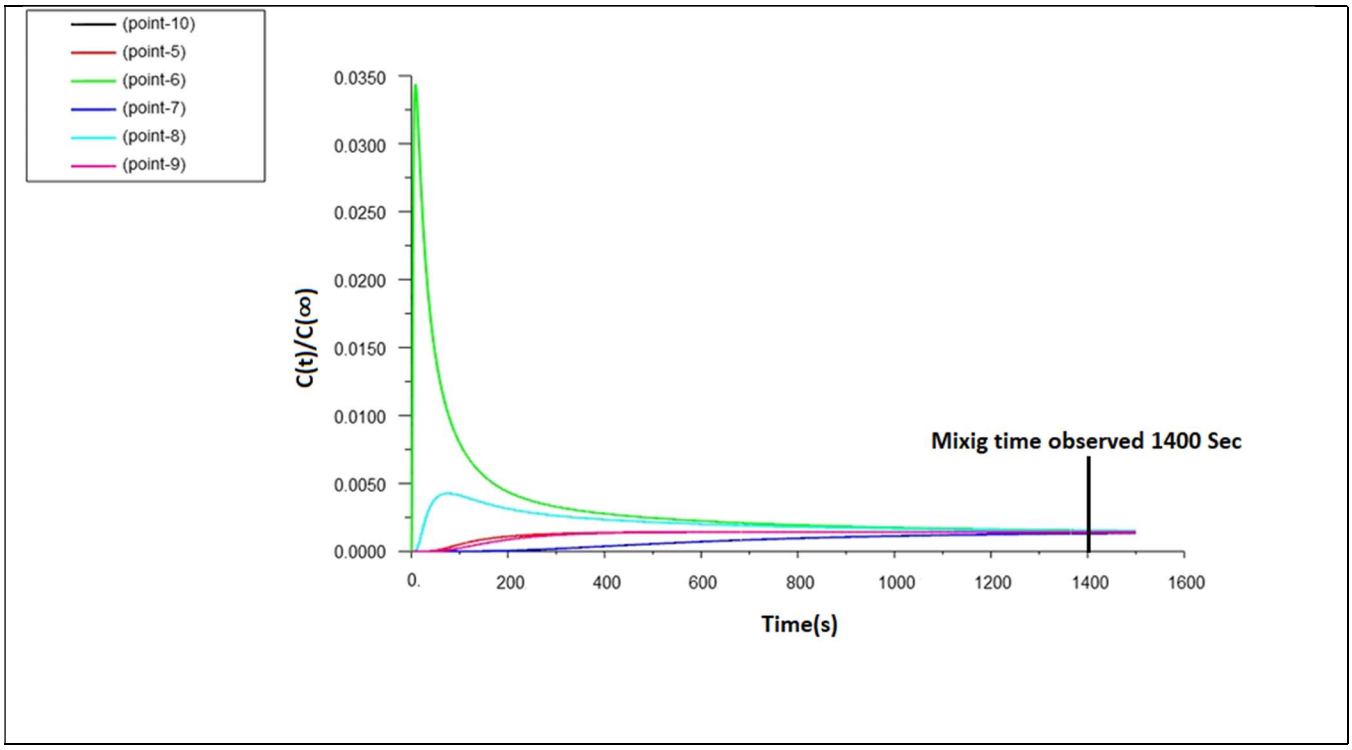

Fig. 6.9c : Mixing time for gas flow rate 4 L/Sec

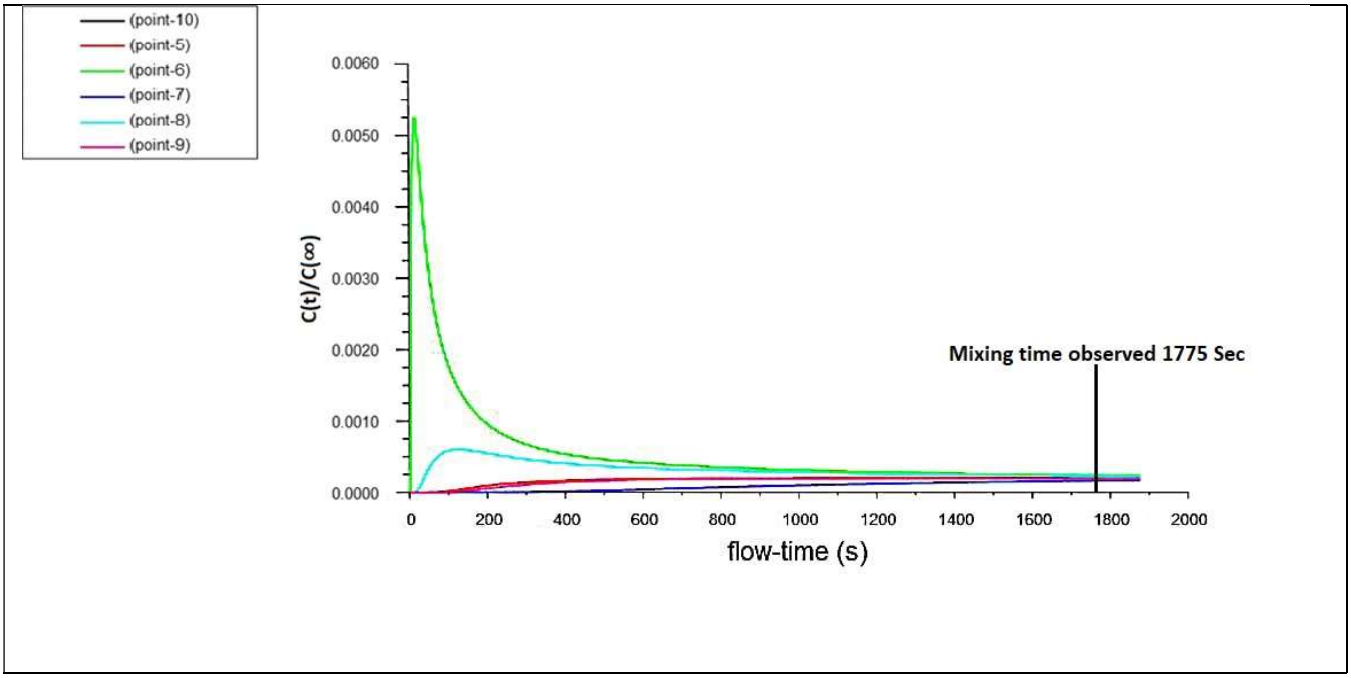

Fig. 6.9d : Mixing time for gas flow rate 2 L/Sec

6.10 Thermal Behaviour of Steel in the Ladle

In the below figure 6.10 it is displayed temperature contour of three different condition in the figure (a) where entered steel temperature 1500^0C. In the model gas have been injecting from bottom of the same and inject gas temperature 300K. Near wall of the model consider insulated boundary and negative heat flux boundary condition apply in outlet of the furnace. In the figure (b) it have been observed that after 120 Sec a temperature gradient create between bottom and top of the furnace due to negative heat flux boundary condition apply in the outlet of the furnace and after 360 Sec thermal homogenization observed.

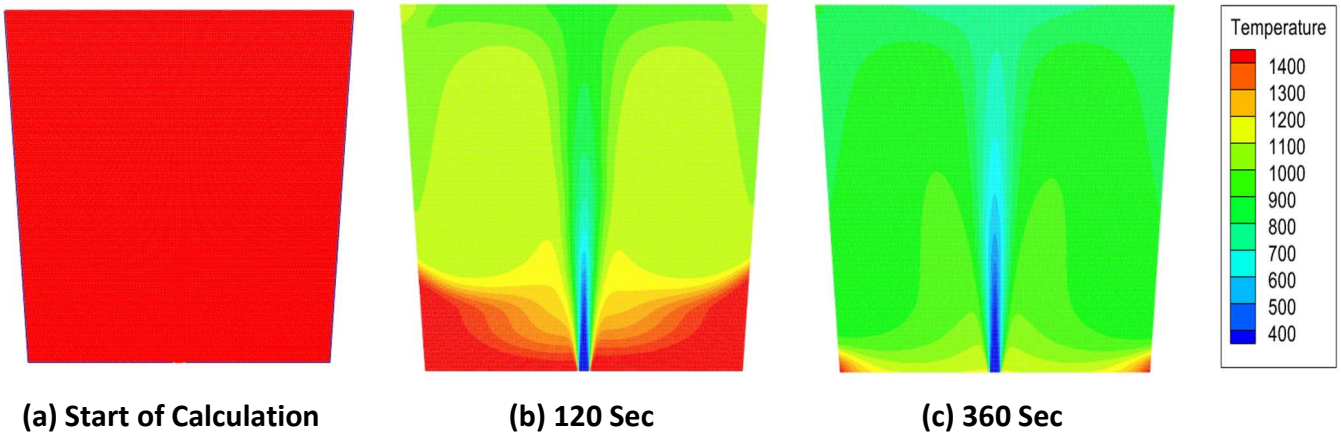

Fig. 6.10: Steel thermal contour

Chapter 7

7.1 Comparison of Different Plug Configurations

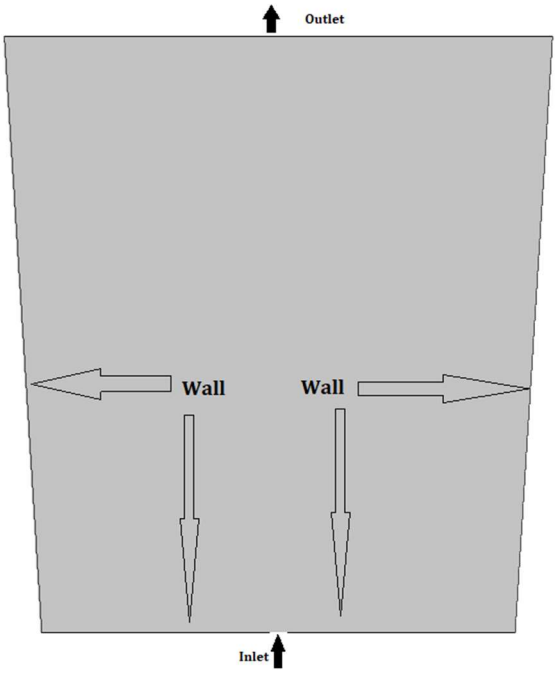

Fig. 7.1a: One Center Plug

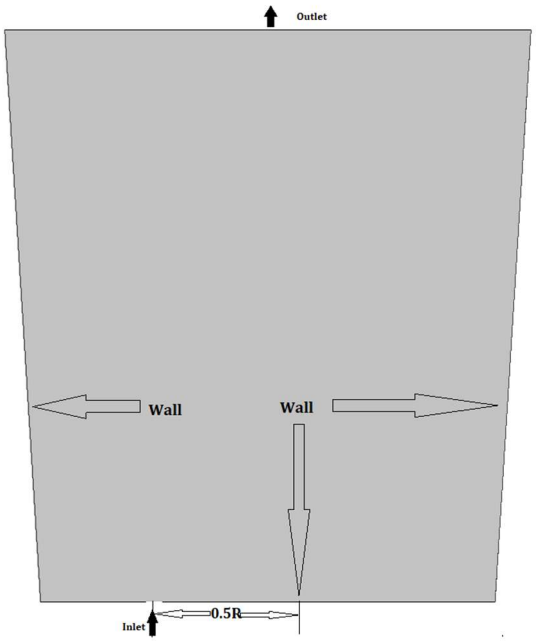

Fig. 7.1b: One Eccentric Plug

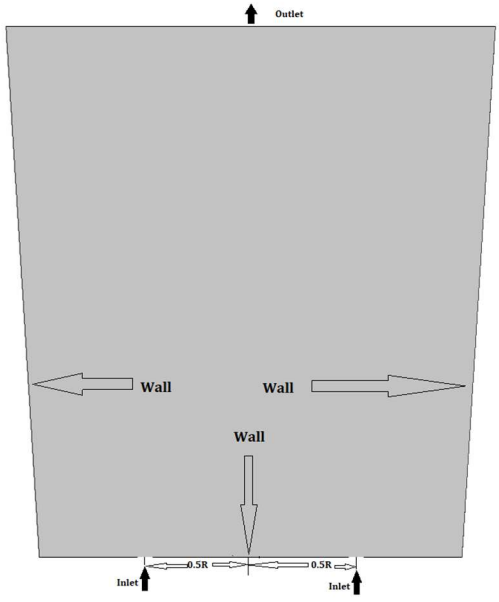

Fig. 7.1c: Two Symmetric Plug

In the indusial ladle bottom plug is provided to inject gas into the ladle which accelerate the mixing process and produce chemically homogenous mixture. In the present study three plugs configurations as per attached figure 7.1a-7.1c provides the arrangements for a one centre plug, with one eccentric plug located at 1/2R distance, and two symmetrical plugs located at 1/2R (R is bottom radius of the ladle) and observed the time to produce homogeneity. In the present study we inject 6L/Sec gas of the different configuration and observed mixing time with the help of species transport model, mean liquid steel velocity and turbulent kinetic energy of the three cases and compared the observation.

7.2 Mixing Behaviour for Different Plug Configurations for Gas Flow Rate 6 L/Sec

In the below figures 7.2a-7.2c shown the comparison the typical variation of the tracer mass concentration of the six monitoring point (P5 to P10) with time of three plug configuration. From the below figure it is observed that for centre plug configuration find out maximum mixing time follow by eccentric plug configuration and for double symmetric plug configuration observed shorten mixing time.

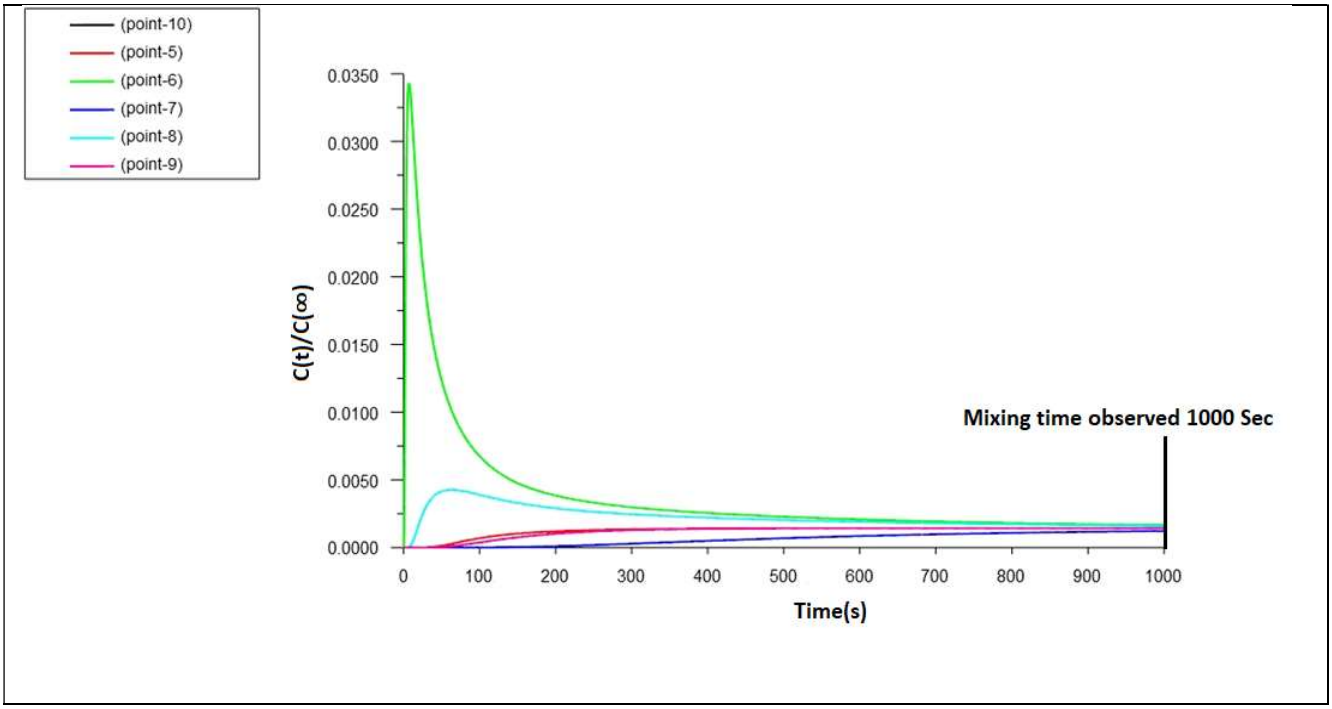

Fig. 7.2a: Mixing time of One Centre plug configuration ladle for gas flow rate 6 L/Sec

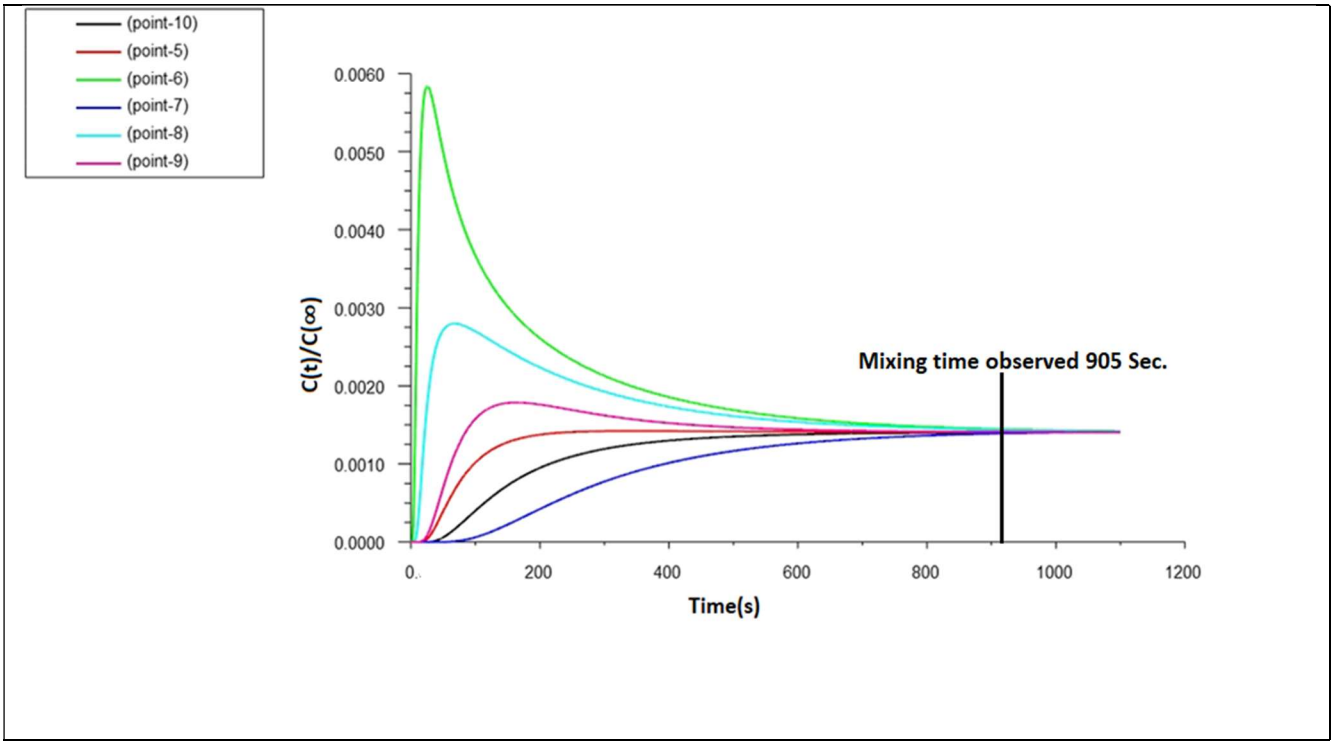

Fig. 7.2b: Mixing time of One eccentric plug configuration ladle for gas flow rate 6 L/Sec

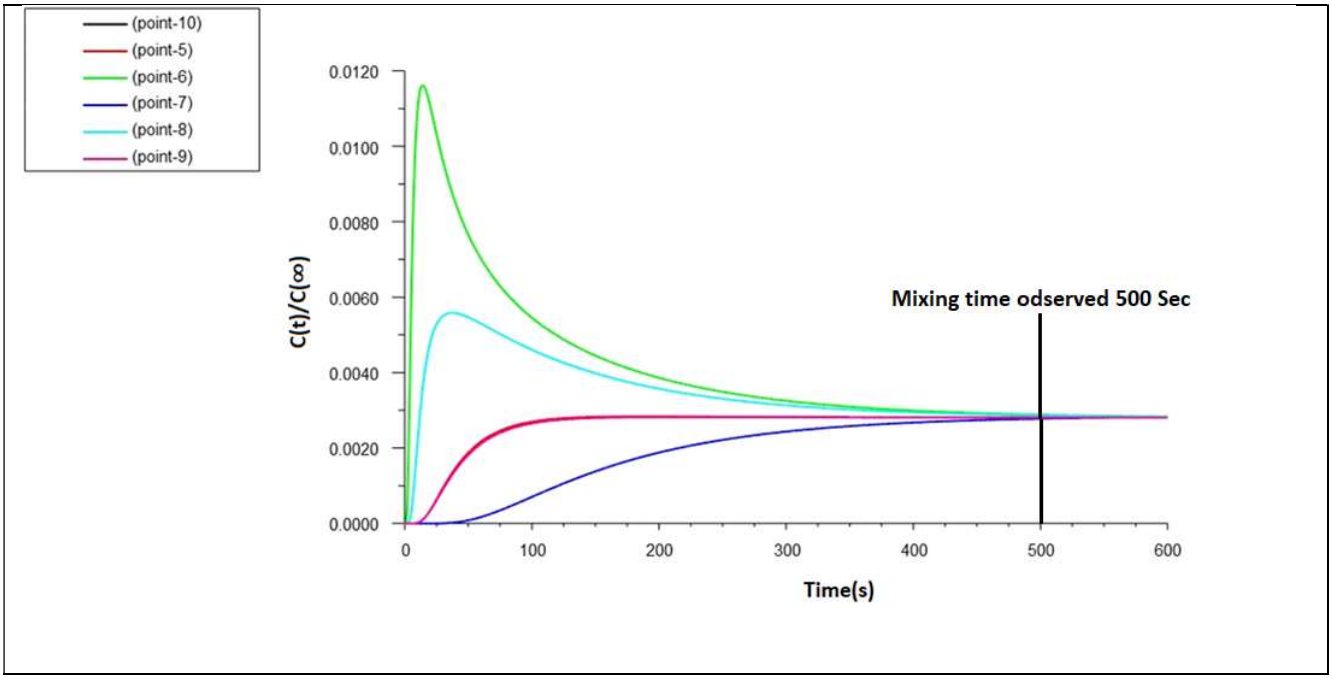

Fig. 7.2c: Mixing time of dual symmetric plug configuration ladle for gas flow rate 6 L/Sec

7.3 Fluid Flow Properties for Different Plug Configurations for Gas Flow Rate 6 L/Sec

Figure 7.3a & 7.3b displayed the mean flow velocity and turbulent kinetics energy of the inside liquid steel. It has been observed that due to two circulations formed [13] between the plug position and ladle wall for one centre and it's more uniform for eccentric plug configuration. In the turbulent kinetics energy, it has been observed that due to more circulation form with respect to the centre plug configuration turbulent kinetics energy of centre plug configuration is little bit more than eccentric plug configuration but due to more stirring energy impart in the double plug configuration mean velocity and turbulent kinetics energy of double symmetric plug configuration is higher than rest other two type configuration.

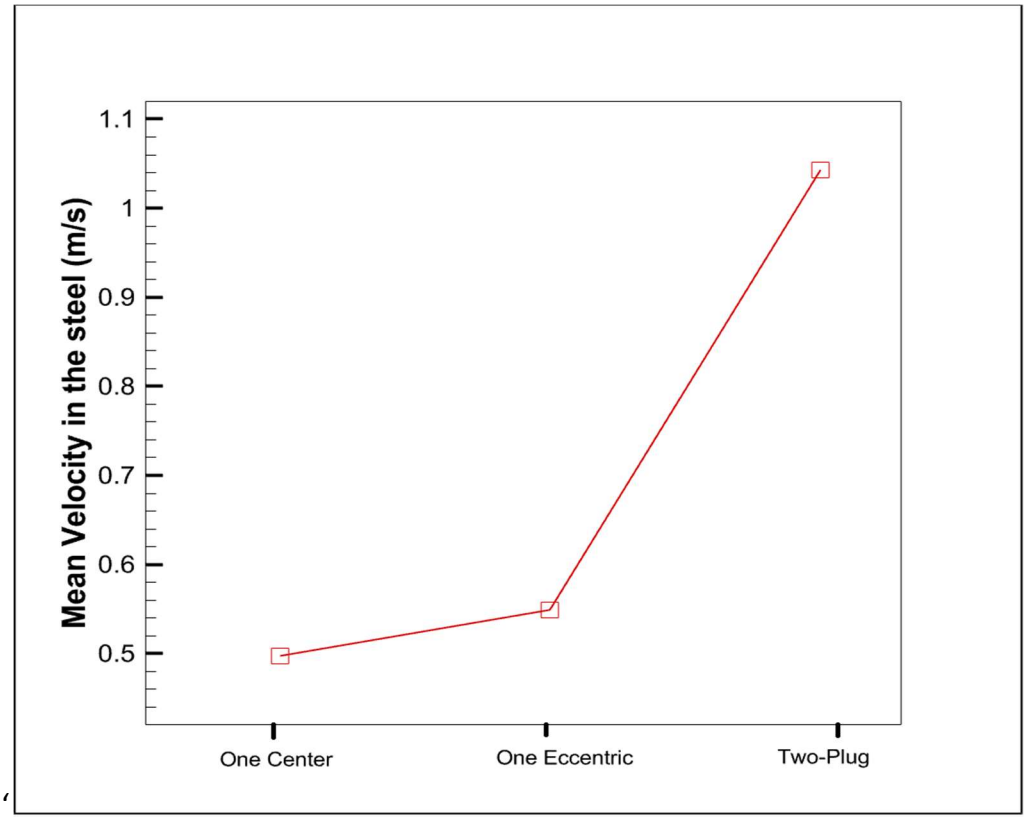

Fig. 7.3a: The predicted mean flow velocity in steel for different plug configurations**.**

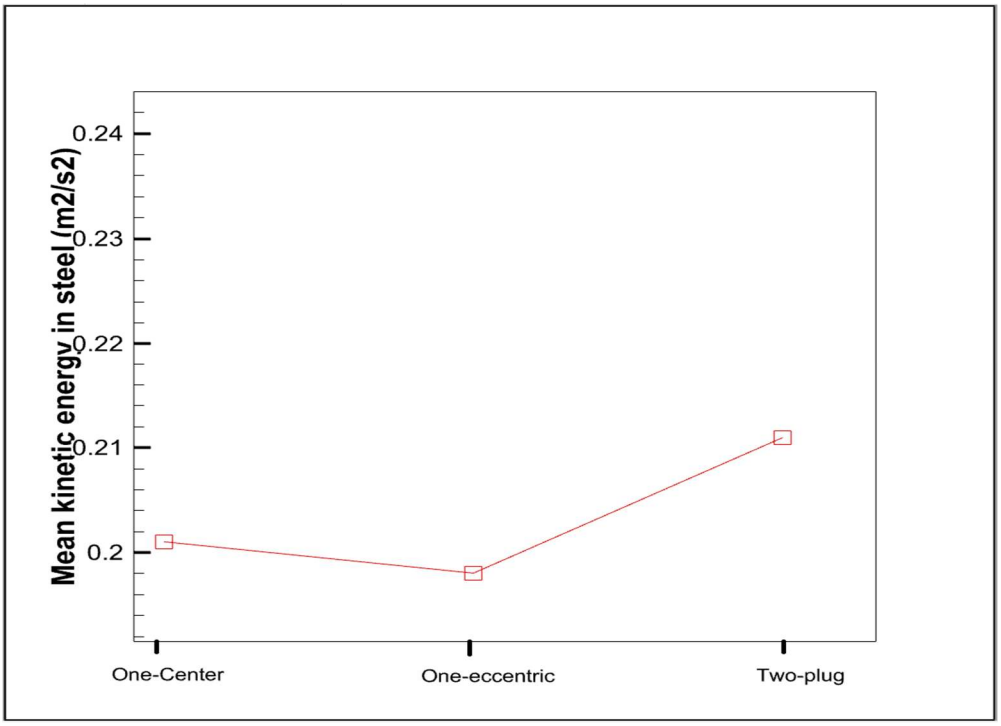

Fig. 7.3b: The predicted turbulent kinetic energy in steel for different plug configurations

Chapter 8

8.1 Conclusion

The Euler-Euler approach have been applied to in the present study to numerical simulate the fluid flow domain and species transport model developed to analysis mixing behaviour in the fluid domain. In the present study we have analysis effect of gas flow rate on fluid velocity, turbulent kinetic energy, turbulent kinetic dissipation rate & mixing time. In the present study also analysis the effect of plug position on fluid velocity, turbulent kinetic energy, turbulent kinetic dissipation rate & mixing time.

So the simulation result concludes the following:

(a) With increase argon gas flow rate fluid velocity, turbulent kinetic energy, turbulent kinetic dissipation rate are increase from bottom of the ladle and then decrease gradually and along the radial direction above parameters suddenly increase at plug position and left and right position of the plug it tends to zero. It's observed from present study that increase gas flow rate mixing time decreased and vice versa.

(b) It's observed that with change plug position fluid velocity, turbulent kinetic energy, turbulent kinetic dissipation rate also changed. In the present study it's observed that minimum value observed from centre plug position and follow by eccentric plug and dual –symmetric plug. Mixing time observed for three plug position and it's observed that centre plug mixing time maximum and follow by eccentric plug and dual-symmetric plug that plug configuration produce homogenous mixture with minimum time.

(C) In the present study it is analysis thermal behaviour of steel in ladle and observed that with time thermal gradient into the ladle decrease for a constant gas flow rate and after a certain time thermal homogeneity observed in the ladle.

Chapter 9

9.1 Scope of Future

The present study only two dimensional numerical base or we can say it theoretical work in two phase transient condition. In the whole study liquid steel consider as incompressible fluid and electromagnetic force can't consider. So in future this study could be continue by applying electromagnetic force, compressible, three phases three dimensional transient model.

Reference

[1]William F Smith , Javad Hashemi , Ravi Prakash, Materials Science and Engineering, McGraw-Hill, Fourth Edition.

[2] Q. Cao, A. Pitts, and L. Nastac: Ironmak. Steelmak., 2016, vol. 12, pp. 1–8.

[3] Liu F, Zhu R, Dong K, et al. ISIJ Int 2015;55:2365–2373.

[4] Haiyan, Tang; Xiaochen, Guo; Guanghui, Wu; Yong, Wang (2016). ISIJ International, 56(12), 2161–2170.

[5] Dai, Weixing; Cheng, Guoguang; Li, Shijian; Huang, Yu; Zhang, Guolei . ISIJ International, (2019)

[6] Urióstegui-Hernández, A.;Garnica-González, P.; Ramos-Banderas, J.Á.;Hernández-Bocanegra, C.A.; Solorio-Díaz, G. Multiphasic. Metals 2021, 11, 1082.

[7] Haiyan, Tang; Xiaochen, Guo; Guanghui, Wu; Yong, Wang (2016. ISIJ International, 56(12), 2161–2170.

[8] M. Chen, N. Wang, Y. Yao, J. Geng and K. Xiong: Steel Res. Int.,78 (2007), 468.

[9] Wei, Rong Zhu, Yun Wang, Kai Dong, Xuetao Wu, Runzao Liu & Fengwu Chen, Ironmaking & Steelmaking(2018)

[10] ANSYS Fluent, 2020 R1. ANSYS Inc. PA, USA

[11] Sarkar, Sandip; Singh, Vikas; Ajmani, Satish Kumar; Singh, Ranjay Kumar; Chacko, Elanjickal Zachariah (2018).ISIJ International, 58(1), 68–77.

[12] Cao, Q., & Nastac, L. (2018). Metallurgical and Materials Transactions B, 49(3), 1388–1404. doi:10.1007/s11663-018-1206-y

[13] Cao, Qing; Nastac, Laurentiu, JOM, (2018), –. doi:10.1007/s11837-018-2977-y

[14] Ramasetti, Eshwar Kumar; Visuri, Ville-Valtteri; Sulasalmi, Petri; Fabritius, Timo; Saatio, Tommi; Li, Mingming; Shao, Lei (2019). Metals, 9(8), 829–841. doi:10.3390/met9080829

[15] Shih, T.; Liou,W.W.; Shabbir, A.; Yang, Z.; Zhu, J. Comput. Fluids 1995, 24, 227–238. [CrossRef]